Check for updates

Extremum Seeking Feedback With Wave Partial Differential Equation Compensation

Tiago Roux Oliveira[1]
Department of Electronics and
Telecommunication Engineering,
State University of Rio de Janeiro (UERJ),
Rio de Janeiro 20550-900, Brazil
e-mail: tiagoroux@uerj.br

Miroslav Krstic
Department of Mechanical and
Aerospace Engineering,
University of California—San Diego (UCSD),
San Diego, CA 92093
e-mail: krstic@ucsd.edu

This paper addresses the compensation of wave actuator dynamics in scalar extremum seeking (ES) for static maps. Infinite-dimensional systems described by partial differential equations (PDEs) of wave type have not been considered so far in the literature of ES. A distributed-parameter-based control law using back-stepping approach and Neumann actuation is initially proposed. Local exponential stability as well as practical convergence to an arbitrarily small neighborhood of the unknown extremum point is guaranteed by employing Lyapunov–Krasovskii functionals and averaging theory in infinite dimensions. Thereafter, the extension for wave equations with Dirichlet actuation, antistable wave PDEs as well as the design for the delay-wave PDE cascade are also discussed. Numerical simulations illustrate the theoretical results.
[DOI: 10.1115/1.4048586]

1 Introduction

Extremum seeking (ES) has been considered one of the main adaptive control strategies to solve real-time optimization problems in a model-free scenario, where the plant may contain both unmodeled dynamics and parametric uncertainties [1].

Despite the large number of ES applications that have emerged in the distinct engineering fields in the recent years (see Refs. [2–5] and references therein), time-delays are listed as a major obstacle in practice, according to the publications [6,7]. The authors of Refs. [6] and [7] have rigorously analyzed the effects of the delays in ES feedback and proposed predictor-based solutions for delay compensation of delayed static and dynamic nonlinear maps. Both gradient and Newton-based designs were studied. Particularly, only pure delays were considered in Refs. [6] and [7], which were represented by a first-order hyperbolic transport partial differential equation (PDE). This infinite-dimensional representation was crucial to allow the generalization of the ES method to different families of PDEs, such as diffusion (heat) processes [8,9] and wider classes of parabolic reaction–advection–diffusion PDEs in Refs. [10] and [11] as well. Although we can check there are many publications in both theory and practice involving stabilization of PDEs [12–17] and time-delay systems [18–21], the topic of ES feedback for PDE-based systems is in its infancy with very few results. None of the references [12–21] has considered the ES approach.

The author in Ref. [12] has developed a boundary stabilizing control that compensates an arbitrarily long delay at the input of an antistable wave equation system. Reference [13] develops an adaptive PDE observer for battery state-of-charge and state-of-health estimation. On the other hand, the authors of Ref. [14] have designed a controller for flow-induced vibrations of an infinite-band membrane. The model of the flow-induced vibration is given by a wave PDE with an antidamping term throughout the one-dimensional domain. The paper [15] presents a deterministic hybrid PDE model which accounts for thermostatically controlled loads populations which facilitates the aggregate synthesis of power control in power networks. Reference [16] deals with the axial vibrations of the cable lifting up a cage with miners via a mining cable. These vibration dynamics can be described by a

coupled wave PDE and an ordinary differential equation (ODE) system with a Neumann interconnection on a time-varying spatial domain. Explicit motion-planning reference solutions are presented for flexible beams with Kelvin–Voigt damping and wave equations in reference [17]. The goal is to generate periodic reference signals for the displacement and deflection angle at the free-end of the beam using only actuation at the base. Publication [18] gives a broad overview of the stability and control of time-delay systems and the paper [19] addresses the challenging adaptive posicast control problem for uncertain systems in the presence of time-delays. The stability of a general class of linear time-invariant-neutral time-delayed systems was studied in Ref. [20], whereas a new analytic approach to obtain the complete solution for systems of delay differential equations based on the concept of Lambert functions was presented in Ref. [21].

In this paper, we extend the class of PDEs for which ES feedback can be employed, by considering *wave dynamics* connected in cascade with the static scalar map to be optimized (see Fig. 1). The tackled problem in the paper is inspired by some specific offshore drilling applications [22] as well as its optimal control [23], where the real-time optimization approach is affected by a wave PDE in the actuation dynamics. The wave process is challenging due to the fact that all of its (infinitely many) eigenvalues are on the imaginary axis, and a limited (finite) speed of propagation (large control amplitudes do not help) [24].

Our paper is the first contribution proposing a novel ES strategy for infinite-dimensional actuation dynamics governed by wave PDEs. The problem studied here is more challenging than the
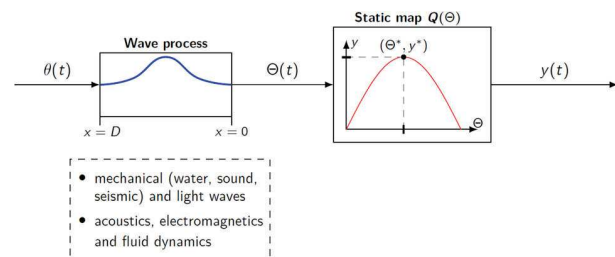

Fig. 1 Cascade of wave PDE with a static map $y(\Theta(t)) = Q(\Theta(t))$. The extremum $y(t) = y^*$ is achieved for $\Theta(t) = \Theta^*$. Wave PDEs are used generally to model different sort of processes such as mechanical, acoustics, electromagnetic, and fluid dynamics.

diffusion case in Refs. [8] and [9] due to another difficulty—the PDE system is second-order in time, which means that the state is "doubly infinite dimensional" (distributed displacement and velocity). This is not so much of a problem dimensionally, as it is a problem in constructing the state transformations for compensating the PDEs [24]. One has to deal with the coupling of two infinite-dimensional states.

The complete control design employing a compensator for the wave actuation dynamics is developed via back-stepping transformation by feeding back the estimates for the gradient and Hessian (first and second derivatives) of the static map to be maximized. Our proofs for local stability of the closed-loop system and the convergence to a small neighborhood of the extremum are based on back-stepping methodology for PDE control [25], the construction of a Lyapunov functional and the use of averaging theorem for infinite-dimensional systems [26]. ES control design for wave PDEs with both Neumann and Dirichlet actuation are considered as well as an antistable wave PDE with boundary antidamping. We also present the design for an antistable wave PDE with input delay [12]. Beyond the complete proofs and new numerical results, these are some of the substantial theoretical differences from our earlier conference version [27]. To the best of our knowledge, all of such results of distributed parameter systems for ES with wave compensation are novel.

1.1 Notation and Terminology.
We denote the partial derivatives of a function $u(x, t)$ as $\partial_x u(x,t) = \partial u(x,t)/\partial x$, $\partial_t u(x,t) = \partial u(x,t)/\partial t$. We conveniently use the compact form $u_x(x,t)$ and $u_t(x,t)$ for the former and the latter, respectively. The two-norm of a finite-dimensional (ODE) state vector $\vartheta(t)$ is denoted by single bars, $|\vartheta(t)|$. In contrast, norms of functions (of x) are denoted by double bars. We denote the spatial $\mathcal{L}_2[0,D]$ norm of the PDE state $u(x, t)$ as $||u(t)||^2_{\mathcal{L}_2([0,D])} := \int_0^D u^2(x,t)dx$, where we drop the index $\mathcal{L}_2([0,D])$ in the following, hence $||\cdot|| = ||\cdot||_{\mathcal{L}_2([0,D])}$, if not otherwise specified. As defined in Ref. [28], a vector function $f(t,\epsilon) \in \mathbb{R}^n$ is said to be of order $\mathcal{O}(\epsilon)$ over an interval $[t_1, t_2]$, if $\exists k, \bar{\epsilon} : |f(t,\epsilon)| \leq k\epsilon, \forall \epsilon \in [0, \bar{\epsilon}]$ and $\forall t \in [t_1, t_2]$. In most cases, we provide no precise estimates for the constants k and $\bar{\epsilon}$, and we use $\mathcal{O}(\epsilon)$ to be interpreted as an order of magnitude relation for sufficiently small ϵ. The definitions of the input-to-state stability (ISS) for ODE-based as well as for PDE-based systems are assumed to be as provided in Refs. [28] and [29], respectively.

2 Motivating Example for Drilling Control

The objective of this motivating part is just to bring a potential connection of the proposed ES strategy to a real-world application, while the main focus of the paper is to pursue designs and a rigorous stability analysis of ES feedback subject to infinite-dimensional actuation dynamics of the wave PDE type.

In this sense, a common type of instability in oil drilling is the friction-induced stick–slip oscillation (see Ref. [22] and references therein), which results in torsional vibrations of the drill-string and can severely damage the drilling facilities (see Fig. 2 from Ref. [23]).

The picture in Fig. 2 shows a modern land-based drilling rig. The tower operates like the derrick of a crane: the traveling block is connected by several steel drill lines with one attached to the deadline anchor and the other being spooled on a drum controlled by AC induction motors. Another electric motor, called Top Drive, is connected to the traveling block. The Top Drive is used to rotate the drill-string, a set of hundreds of drill pipes (about 30 ft long each) that conducts the bore hole drilling assembly (BHA). The BHA contains several sensors (pressure, temperature, and vibration among others) and the drill bit itself. There are several different types of drill bit design and materials, adequate for drilling different geological formations.

In analogy, the rig operates similarly to a drill press, but with drill bit which is several inches wide (4 in. to 36 in. is a common range) and up to several miles long (an onshore well can be as
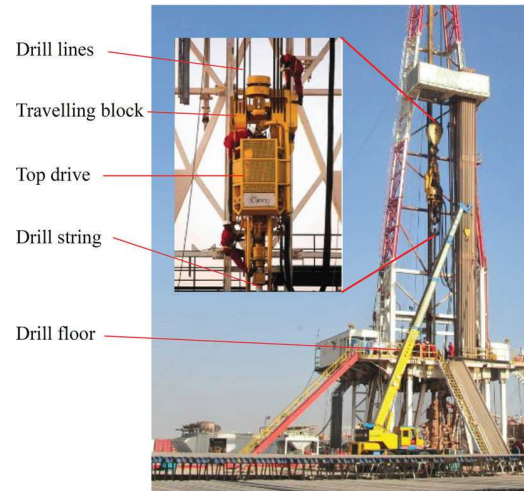

Fig. 2 Picture showing the topside of a drilling rig [23]

shallow as 200 yards or as deep as 2 miles). By rotating this drill-string and using its weight to generate an axial force, the BHA mills the rocks, drilling the well. Because of the small diameter when compared to its length, the drill-string is subject to axial and torsional effects, much like a flexible rod. Because of this elasticity, the force and velocity propagation can be modeled by *wave equations*.

In this particular model, the actuation is the velocity of the traveling block, i.e., the axial velocity of the drill-string on the surface. Although not represented here, the rotational velocity also influences the rate of penetration (ROP) in a real scenario. The model output is the weight on hook which somewhat models the weight on bit (WOB). The WOB estimates the contact between the drill bit and the rock formation and it is the downhole boundary condition to be controlled. In Ref. [23], the authors have discussed the feasibility of controlling the hook load to optimize ROP while drilling.

The key point that enables such an approach is the concept of bit foundering [23], i.e., the fact that ROP tapers off (and sometimes starts decreasing) with increasing weight on bit past the foundering point. This makes the static mapping between ROP and weight on bit upward convex in an interval around the foundering point. This transfers to an upward convex static mapping between the equilibrium hook load set point and feed rate. Consequently, these signals can be used as the plant input and output for the design of a drilling control system. Hence, this physical application motivates our ES scheme for static maps with actuation dynamics described by wave PDEs, as depicted in Fig. 1.

3 Problem Formulation

We start our presentation in Sec. 3.1 recalling the basic results of gradient-based ES for static maps (free of PDEs) and then we move on to our more general framework in Sec. 3.2 where wave PDEs are considered in the input of the static maps we want to optimize in real-time.

3.1 Basic Extremum Seeking for Static Maps.
In the simplest case of ES for static maps, the goal is to find and maintain the optimum of an unknown nonlinear static map $Q(\cdot)$ with optimal unknown output y^*, unknown optimizer θ^*, measurable output y and input θ. Without loss of generality, we consider maximization problems. The method of sinusoidal perturbation [1] varies the input parameter θ of the static map to obtain an estimate of the gradient G for the static map. Hence, the additive dither $S(t) = a\sin(\omega t)$, with amplitude a and frequency ω, is added to the estimation of the optimizer θ^*, given by $\hat{\theta}$. The multiplicative

dither signal to estimate the gradient of the static map is chosen as $M(t) = \frac{2}{a}\sin(\omega t)$. The idea of choosing the dither signals above as well as the adaptation law $\dot{\hat{\theta}}(t) = kG(t)$ is to achieve the averaged signal of the gradient estimate G given by $G_{\mathrm{av}}(t) = H\tilde{\theta}_{\mathrm{av}}$ $= H(\hat{\theta}_{\mathrm{av}} - \theta^*)$, where H is the unknown negative Hessian of the static map and $\tilde{\theta} = \hat{\theta} - \theta^*$ the estimation error. This yields to the averaged error dynamics $\dot{\tilde{\theta}}_{\mathrm{av}} = KH\tilde{\theta}_{\mathrm{av}}$, with adaption gain $K > 0$. The average system is exponentially stable and by the averaging theorem in Ref. [28], the original error dynamics is exponential stable with respect to a small residual set.

3.2 Wave Partial Differential Equation Under Neumann Actuation.

We consider actuation dynamics which are described by a *wave* (PDE) *process*, where the actuator $\theta(t)$ and the propagated actuator $\Theta(t)$ are given by

$$\Theta(t) = \partial_x \alpha(0,t) \tag{1}$$

$$\partial_{tt}\alpha(x,t) = \partial_{xx}\alpha(x,t), \quad x \in [0,D] \tag{2}$$

$$\alpha(0,t) = 0 \tag{3}$$

$$\partial_x \alpha(D,t) = \theta(t) \tag{4}$$

with the domain length D being arbitrary, but known.

The Neumann actuation choice $\partial_x \alpha(D,t) = \theta(t)$ is first pursued because this is a natural physical choice since $\partial_x \alpha(D,t)$ corresponds to a force on the string's boundary. In Sec. 6, we address the case of an alternative actuation choice, Dirichlet actuation via $\alpha(D,t) = \theta(t)$.

The measurement is defined by the unknown static map with input (1), such that

$$y(t) = Q(\Theta(t)) \tag{5}$$

For the sake of simplicity, we assume the following.

ASSUMPTION 1. *The unknown nonlinear static map is locally quadratic*, i.e.,

$$Q(\Theta) = y^* + \frac{H}{2}(\Theta - \Theta^*)^2 \tag{6}$$

in the neighborhood of the extremum, where besides $\Theta^* \in \mathbb{R}$ and $y^* \in \mathbb{R}$ being unknown, the scalar $H < 0$ is the unknown Hessian of the static map.

Hence, the output of the static map is given by

$$y(t) = y^* + \frac{H}{2}(\Theta(t) - \Theta^*)^2 \tag{7}$$

Combining the above actuation dynamics and the basic ES scheme, further adapting the proposed formulation based on PDEs in Ref. [6], the closed-loop ES with actuation dynamics governed by a wave PDE system under a boundary PDE control is shown in Fig. 3.
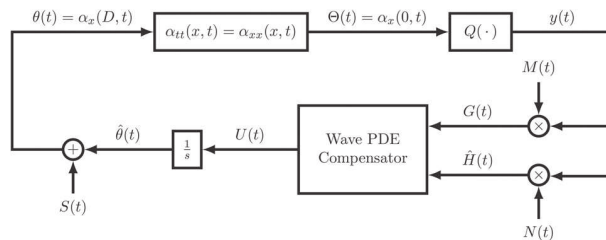

Fig. 3 Gradient ES with actuation dynamics governed by a wave PDE with compensating controller (40), additive and multiplicative perturbation signals (23), (26), and (27), respectively

3.3 System and Signals.

As in the basic ES scheme, we define the unknown optimal input θ^* of $\theta(t)$ with respect to the static map and the wave process, with the relation $\Theta^* = \theta^*$. Since our goal is to find the unknown optimal input θ^*, we define the estimation error

$$\tilde{\theta}(t) := \hat{\theta}(t) - \theta^* \tag{8}$$

where $\hat{\theta}(t)$ is the estimate of θ^*. To make Eq. (8) consistent with the optimizer of the static map Θ^*, we introduce the propagated estimation error $\vartheta(t) := \bar{\Theta}(t) - \Theta^*$ through the wave PDE domain

$$\vartheta(t) := \partial_x \bar{\alpha}(0,t) \tag{9}$$

$$\partial_{tt}\bar{\alpha}(x,t) = \partial_{xx}\bar{\alpha}(x,t), \quad x \in [0,D] \tag{10}$$

$$\bar{\alpha}(0,t) = 0 \tag{11}$$

$$\partial_x \bar{\alpha}(D,t) = \tilde{\theta}(t) \tag{12}$$

From the control loop in Fig. 3, we get

$$\dot{\hat{\theta}}(t) = U(t) \tag{13}$$

Taking the time derivative of Eqs. (9)–(12) and with the help of Eqs. (8) and (13), the propagated error dynamics is written as the following cascade of a wave PDE and ODE (integrator) with Neumann interconnection [30]:

$$\dot{\vartheta}(t) = \partial_x u(0,t) \tag{14}$$

$$\partial_{tt}u(x,t) = \partial_{xx}u(x,t), \quad x \in [0,D] \tag{15}$$

$$u(0,t) = 0 \tag{16}$$

$$\partial_x u(D,t) = U(t) \tag{17}$$

where $\dot{\tilde{\theta}}(t) = \dot{\hat{\theta}}(t)$, since θ^* is constant, and

$$u(x,t) = \partial_t \bar{\alpha}(x,t) \tag{18}$$

As in extremum seeking without actuation through a wave PDE domain, the perturbation signal $S(t)$ should add $a\sin(\omega t)$ to $\Theta(t)$, thus compensating the wave process. Hence, $a\sin(\omega t)$ with perturbation amplitude a and frequency ω is applied as follows:

$$S(t) := \partial_x \beta(D,t) \tag{19}$$

$$\partial_{tt}\beta(x,t) = \partial_{xx}\beta(x,t), \quad x \in [0,D] \tag{20}$$

$$\beta(0,t) = 0 \tag{21}$$

$$\partial_x \beta(0,t) = a\sin(\omega t) \tag{22}$$

Equations (19)–(22) describe a trajectory generation problem as in chapter 12 of Ref. [25]. The explicit solution of Eq. (19) is given by

$$S(t) = a\cos(\omega D)\sin(\omega t) \tag{23}$$

since $\beta(x,t) = \frac{a}{\omega}\sin(\omega x)\sin(\omega t)$. The relation among the propagated estimation error $\vartheta(t)$, the propagated input $\Theta(t)$, and the optimizer of the static map Θ^* is given by

$$\vartheta(t) + a\sin(\omega t) = \Theta(t) - \Theta^* \tag{24}$$

which can be easily proven since

$$\bar{\alpha}(x,t) = \alpha(x,t) - \beta(x,t) - \Theta^* \tag{25}$$

for $x = D$, and considering $\theta(t) = \hat{\theta}(t) + S(t)$ along with the solutions of Eqs. (1)–(4), (9)–(12), and (19)–(22). It remains to define the dither signal $N(t)$ which is used to estimate the Hessian of the static map by multiplying it with the output $y(t)$ of the static map. In Ref. [31], the Hessian estimate is derived as

$$\hat{H}(t) = N(t)y(t) \quad \text{with} \quad N(t) = -\frac{8}{a^2}\cos(2\omega t) \qquad (26)$$

Note that the dither signal $M(t)$, employed to estimate the gradient, is the same as in the basic ES (see Sec. 3.1), such that

$$G(t) = M(t)y(t) \quad \text{with} \quad M(t) = \frac{2}{a}\sin(\omega t) \qquad (27)$$

4 Controller Design and Closed-Loop System

In this section, we present the proposed filtered boundary control with perturbation-based (averaging-based) estimates of the gradient and Hessian used for wave compensation in the closed-loop extremum seeking feedback of Fig. 3.

4.1 Wave Compensation by Means of Hessian's Estimation.
We consider the PDE–ODE cascade (14)–(17). As in Ref. [30], we use the back-stepping transformation

$$w(x,t) = u(x,t) - \int_0^x l(x,\sigma)u_t(\sigma,t)d\sigma - \gamma(x)\vartheta(t) \qquad (28)$$

with the gain kernels

$$l(x,\sigma) = \gamma(x - \sigma) \qquad (29)$$

$$\gamma(x) = \bar{K}[0\ I]e^{Ax}[I\ 0]^T, \quad A = \begin{pmatrix} 0 & 0 \\ I & 0 \end{pmatrix} \qquad (30)$$

which transforms (14)–(17) into the target system

$$\dot{\vartheta}(t) = \bar{K}\vartheta(t) + w_x(0,t), \quad \bar{K} < 0 \qquad (31)$$

$$\partial_{tt}w(x,t) = \partial_{xx}w(x,t), \quad x \in [0,D] \qquad (32)$$

$$w(0,t) = 0 \qquad (33)$$

$$w_x(D,t) = -\bar{c}w_t(D,t), \quad \bar{c} > 0 \qquad (34)$$

Since the target system (31)–(34) is exponentially stable, the controller which compensates the wave process can be obtained by evaluating the back-stepping transformation (28) at $x = D$ as

$$U(t) = \bar{c}[\bar{K}u(D,t) - \partial_t u(D,t)] + \rho(D)\vartheta(t)$$
$$+ \int_0^D \rho(D-\sigma)\partial_t u(\sigma,t)d\sigma \qquad (35)$$

where $\rho(s) = \bar{K}[0\ I]e^{As}[0\ I]^T$. However, the proposed control law in Eq. (35) is not applicable directly, because we have no measurement on $\vartheta(t)$. Thus, we introduce an important result of Ref. [31]: the averaged version of the gradient (27) and Hessian (26) estimates are

$$G_{\mathrm{av}}(t) = H\vartheta_{\mathrm{av}}(t), \quad \hat{H}_{\mathrm{av}}(t) = H \qquad (36)$$

if a quadratic map as in Eq. (6) is considered. For the proof of Eq. (36), see Ref. [31]. Regarding Eq. (36), we average Eq. (35) and choose $\bar{K} = KH$ with $K > 0$, such that

$$U_{\mathrm{av}}(t) = \bar{c}[KHu_{\mathrm{av}}(D,t) - \partial_t u_{\mathrm{av}}(D,t)] + \bar{\rho}(D)KH\vartheta_{\mathrm{av}}(t)$$
$$+ KH\int_0^D \bar{\rho}(D-\sigma)\partial_t u_{\mathrm{av}}(\sigma,t)d\sigma \qquad (37)$$

with

$$\bar{\rho}(s) = [0\ I]e^{As}[0\ I]^T, \quad A = \begin{pmatrix} 0 & 0 \\ I & 0 \end{pmatrix} \qquad (38)$$

By plugging the averaged estimate (36) into Eq. (37), we obtain

$$U_{\mathrm{av}}(t) = \bar{c}[KHu_{\mathrm{av}}(D,t) - \partial_t u_{\mathrm{av}}(D,t)] + \bar{\rho}(D)KG_{\mathrm{av}}(t)$$
$$+ KH\int_0^D \bar{\rho}(D-\sigma)\partial_t u_{\mathrm{av}}(\sigma,t)d\sigma \qquad (39)$$

Due to technical reasons in the application of the averaging theorem for infinite-dimensional systems [26] in the stability proof, we introduce a low-pass filter to the controller so that $U(t)$ can be treated as a state variable. Finally, we get the average-based infinite-dimensional control law to compensate the wave process

$$U(t) = \frac{c}{s+c}\left\{\bar{c}[K\hat{H}(t)u(D,t) - \partial_t u(D,t)] + \bar{\rho}(D)KG(t)\right.$$
$$\left. + K\hat{H}(t)\int_0^D \bar{\rho}(D-\sigma)\partial_t u(\sigma,t)d\sigma\right\} \qquad (40)$$

where $c > 0$ is chosen later. For notation convenience, we mix the time and frequency domain in Eq. (40), where the low-pass filter acts as an operator on the term between braces.

4.2 Closed-Loop System.
Substituting Eq. (40) into Eq. (17), we can write the closed-loop system (14)–(17) as

$$\dot{\vartheta}(t) = \partial_x u(0,t) \qquad (41)$$

$$\partial_{tt}u(x,t) = \partial_{xx}u(x,t), \quad x \in [0,D] \qquad (42)$$

$$u(0,t) = 0 \qquad (43)$$

$$\partial_x u(D,t) = \frac{c}{s+c}\left\{\bar{c}[K\hat{H}(t)u(D,t) - \partial_t u(D,t)] + \bar{\rho}(D)KG(t)\right.$$
$$\left. + K\hat{H}(t)\int_0^D \bar{\rho}(D-\sigma)\partial_t u(\sigma,t)d\sigma\right\} \qquad (44)$$

The availability of Lyapunov functionals via back-stepping transformation [25] permits the stability analysis in the next section of the complete feedback system (41)–(44) with a representation of the form of cascade ODE–PDE equations and the infinite-dimensional control law.

5 Stability Analysis

The following theorem provides the stability and local convergence properties of the closed-loop system.

THEOREM 1. *Consider the system in Fig. 3 with the dynamic system being represented by the nonlinear quadratic map (7), satisfying Assumption 1, in cascade with the actuation dynamics governed by the wave PDE in Eqs. (1)–(4). For a sufficiently large $c > 0$, there exists some $\bar{\omega}(c) > 0$, such that $\forall \omega > \bar{\omega}$, the closed-loop system (41)–(44) with states $\vartheta(t)$, $u(x,t)$, has an unique locally exponentially stable periodic solution in t of period $\Pi := 2\pi/\omega$, denoted by $\vartheta^\Pi(t)$, $u^\Pi(x,t)$, satisfying $\forall t \geq 0$*

$$(|\vartheta^\Pi(t)|^2 + ||\partial_x u^\Pi(t)||^2 + ||\partial_t u^\Pi(t)||^2$$
$$+ |\partial_x u^\Pi(D,t)|^2)^{1/2} \leq \mathcal{O}(1/\omega) \qquad (45)$$

Furthermore

$$\limsup_{t\to\infty} |\theta(t) - \theta^*| = \mathcal{O}(a + 1/\omega) \qquad (46)$$

$$\limsup_{t\to\infty} |\Theta(t) - \Theta^*| = \mathcal{O}(a + 1/\omega) \qquad (47)$$

$$\limsup_{t\to\infty} |y(t) - y^*| = \mathcal{O}(a^2 + 1/\omega^2) \qquad (48)$$

Proof. The proof is structured into Steps 1–6, analogously to what has been done in Ref. [8].

5.1 Step 1: Average Closed-Loop System. The average version of the system (41)–(44) for ω large is

$$\dot{\vartheta}_{\mathrm{av}}(t) = \partial_x u_{\mathrm{av}}(0,t) \qquad (49)$$

$$\partial_{tt} u_{\mathrm{av}}(x,t) = \partial_{xx} u_{\mathrm{av}}(x,t), \quad x \in [0, D] \qquad (50)$$

$$u_{\mathrm{av}}(0,t) = 0 \qquad (51)$$

$$\frac{d}{dt} \partial_x u_{\mathrm{av}}(D,t) = -c\partial_x u_{\mathrm{av}}(D,t) - c\Big[\bar{c}[KHu_{\mathrm{av}}(D,t) - \partial_t u_{\mathrm{av}}(D,t)]$$
$$+ \bar{\rho}(D)KH\vartheta_{\mathrm{av}}(t) + KH\int_0^D \bar{\rho}(D-\sigma)\partial_t u_{\mathrm{av}}(\sigma,t)d\sigma\Big] \qquad (52)$$

where the low-pass filter is represented in the state-space form.

5.2 Step 2: Back-Stepping Transformation Into Target System. With some abuse of notation we also use $w(x, t)$ to denote the average transformed state. From Eq. (28), the back-stepping transformation

$$w(x,t) = u_{\mathrm{av}}(x,t)$$
$$- \int_0^x \gamma(x-\sigma)\partial_t u_{\mathrm{av}}(\sigma,t)d\sigma - \gamma(x)\vartheta_{\mathrm{av}}(t) \qquad (53)$$

maps the average closed-loop system (49)–(52) into the exponentially stable target system (shown in Step 3)

$$\dot{\vartheta}_{\mathrm{av}}(t) = KH\vartheta_{\mathrm{av}}(t) + w_x(0,t) \qquad (54)$$

$$\partial_{tt}w(x,t) = \partial_{xx}w(x,t), \quad x \in [0, D] \qquad (55)$$

$$w(0,t) = 0 \qquad (56)$$

$$w_t(D,t) = -\frac{1}{\bar{c}}\partial_x w(D,t), \quad \bar{c} > 0 \qquad (57)$$

$$\partial_x w(D,t) = -\frac{1}{c}\partial_t\partial_x u_{\mathrm{av}}(D,t) \qquad (58)$$

The target system (54)–(58) can be derived by plugging the inverse back-stepping transformation [30]

$$u_{\mathrm{av}}(x,t) = w(x,t) + KHn(x)\vartheta_{\mathrm{av}}(t)$$
$$+ KH\int_0^x n(x-\sigma)w_t(\sigma,t)d\sigma \qquad (59)$$

with

$$n(x) = [0\ I]e^{\bar{A}x}[I\ 0]^T, \quad \bar{A} = \begin{pmatrix} 0 & (KH)^2 \\ I & 0 \end{pmatrix} \qquad (60)$$

into the average closed-loop system (49)–(52). Additionally taking the time derivative of the back-stepping transformation (53) along with Eq. (52) and its inverse (59), we arrive at Eq. (58) reminding that $\dot{U}_{\mathrm{av}}(t) = \partial_t\partial_x u_{\mathrm{av}}(D,t)$, or equivalently

$$\partial_t w_x(D,t) = -cw_x(D,t) + KHw(D,t)$$
$$+ (KH)^2 n(D)\vartheta_{\mathrm{av}}(t) + (KH)^2\int_0^D n(D-\sigma)w_t(\sigma,t)d\sigma \qquad (61)$$

5.3 Step 3: Exponential Stability of the Target System. We start by introducing the system norms

$$\Omega(t) = ||\partial_x u_{\mathrm{av}}(t)||^2 + ||\partial_t u_{\mathrm{av}}(t)||^2 + |\vartheta_{\mathrm{av}}(t)|^2 + |\partial_x u_{\mathrm{av}}(D,t)|^2 \qquad (62)$$

$$\Xi(t) = ||w_x(t)||^2 + ||w_t(t)||^2 + |\vartheta_{\mathrm{av}}(t)|^2 + |w_x(D,t)|^2 \qquad (63)$$

To prove the stability of the closed-loop system, we consider the Lyapunov–Krasovskii functional

$$V(t) = \frac{\vartheta_{\mathrm{av}}^2(t)}{2} + \bar{a}E(t) + \frac{b}{2}w_x^2(D,t) \qquad (64)$$

where the parameters $\bar{a}, b > 0$ are to be chosen later and the functional $E(t)$ is defined by [30]

$$E(t) = \frac{1}{2}\big(||w_x(t)||^2 + ||w_t(t)||^2\big)$$
$$+ \delta\int_0^D (1+y)w_x(y,t)w_t(y,t)dy \qquad (65)$$

where $\delta > 0$ is also a parameter to be chosen later. We observe that

$$\theta_1\Xi \le V \le \theta_2\Xi \qquad (66)$$

where

$$\theta_1 = \min\left\{\frac{1}{2}, \frac{\bar{a}}{2}[1 - \delta(1+D)], \frac{b}{2}\right\} \qquad (67)$$

$$\theta_2 = \min\left\{\frac{1}{2}, \frac{\bar{a}}{2}[1 + \delta(1+D)], \frac{b}{2}\right\} \qquad (68)$$

We choose

$$0 < \delta < \frac{1}{1+D} \qquad (69)$$

in order to ensure that θ_1 and θ_2 are non-negative and so the Lyapunov function V in Eq. (64) is positive definite. Next, we compute the time derivative of $E(t)$

$$\dot{E}(t) = -\frac{\delta}{2}\Big[||w_x(t)||^2 + ||w_t(t)||^2 + w_x(0,t)^2\Big]$$
$$+ \frac{\delta}{2}(1+D)\Big[w_t(D,t)^2 + w_x(D,t)^2\Big]$$
$$+ w_x(D,t)w_t(D,t) \qquad (70)$$

From Eq. (57), we substitute $w_x(D,t) = -\bar{c}w_t(D,t)$ into Eq. (70) and get

$$\dot{E}(t) = -\frac{\delta}{2}\Big[||w_x(t)||^2 + ||w_t(t)||^2 + w_x(0,t)^2\Big]$$
$$- \Big[\bar{c} - \delta\frac{1+D}{2}(1+\bar{c}^2)\Big]w_t(D,t)^2 \qquad (71)$$

Choosing now

$$\delta < \frac{2\bar{c}}{(1+D)(1+\bar{c}^2)} \qquad (72)$$

we have that the constant between brackets in the second term of Eq. (71) is positive. Now, computing the complete derivative of $V(t)$, associated with the solution of the target system (54)–(58), we have

$$\dot{V}(t) = KH\vartheta_{\mathrm{av}}^2(t) + \vartheta_{\mathrm{av}}(t)w_x(0,t) \\ + \bar{a}\dot{E}(t) + bw_x(D,t)\partial_t w_x(D,t) \tag{73}$$

By applying Young's inequality to the second term in Eq. (73), we can write

$$\dot{V}(t) \leq \frac{KH}{2}\vartheta_{\mathrm{av}}^2(t) + \left[\frac{1}{2|KH|} - \bar{a}\frac{\delta}{2}\right]w_x(0,t)^2 \\ - \bar{a}\frac{\delta}{2}\left[||w_x(t)||^2 + ||w_t(t)||^2\right] + bw_x(D,t)\partial_t w_x(D,t) \tag{74}$$

By choosing

$$\bar{a} \geq \frac{1}{\delta|KH|} \tag{75}$$

we now obtain

$$\dot{V}(t) \leq \frac{KH}{2}\vartheta_{\mathrm{av}}^2(t) - \bar{a}\frac{\delta}{2}\left[||w_x(t)||^2 + ||w_t(t)||^2\right] \\ + bw_x(D,t)\partial_t w_x(D,t) \tag{76}$$

Rigorously, substituting Eq. (61) into (76), the last term in the right-hand side of Eq. (76) can be treated analogously to what have been done in references [8] and [9] for diffusion processes or even as carried out in Ref. [6] with pure delays, when the parameter $c > 0$ is assumed sufficiently large. The first term $-cw_x(D,t)$ in the right-hand side of Eq. (61) when plugged to Eq. (76) results in $-bcw_x^2(D,t)$. Intuitively, $w_x(D,t) \to 0$ as $c \to +\infty$ according to Eq. (58) since $w_x(x,t)$ is at least bounded from Eq. (71) and, consequently, Eq. (76) becomes negative definite. After lengthy calculations, applying Young's, Poincare's, Agmon's, and Cauchy–Schwarz's inequalities (more than one) and with the help of integration by parts, we conclude that there exists $c^* > 0$ (depending on KH and D) such that, for $c > c^*$ sufficiently large in Eq. (40), one has

$$\dot{V}(t) \leq -\eta V(t), \quad \eta > 0 \tag{77}$$

and the target system (54)–(58) is exponentially stable in the norm

$$\left(|\vartheta_{\mathrm{av}}(t)|^2 + ||w_x(t)||^2 + ||w_t(t)||^2 + |w_x(D,t)|^2\right)^{1/2}$$

i.e., in the transformed variables $(\vartheta_{\mathrm{av}}, w)$.

5.4 Step 4: Exponential Stability Estimate ($\mathcal{H}_1$) of the Average Closed-Loop System.
In the last step, we arrive at the estimate

$$V(t) \leq e^{-\eta t}V(0), \quad \eta > 0 \tag{78}$$

In order to prove stability of the closed-loop system in its original variables $(\vartheta_{\mathrm{av}}, u_{\mathrm{av}})$ from Eq. (78), we provide inequalities relating the variables $u(x,t)$ and $w(x,t)$. From the inverse transformation (59), we obtain that

$$\partial_x u_{\mathrm{av}}(x,t) = w_x(x,t) + \int_0^x \phi'(x-y)w(y,t)dy \\ + \int_0^x n'(x-y)w_t(y,t)dy + \psi(x)'\vartheta_{\mathrm{av}}(t) \tag{79}$$

$$\partial_t u_{\mathrm{av}}(x,t) = w_t(x,t) + \int_0^x \phi(x-y)w_t(y,t)dy \\ + \int_0^x n'(x-y)w(y,t)dy + \psi(x)KH\vartheta_{\mathrm{av}}(t) \tag{80}$$

Applying Poincare's, Young's, and the Cauchy–Schwartz inequalities, we get

$$||\partial_x u_{\mathrm{av}}(t)||^2 \leq \alpha_1||w_x(t)||^2 + \alpha_2||w_t(t)||^2 + \alpha_3|\vartheta_{\mathrm{av}}(t)|^2 \\ ||\partial_t u_{\mathrm{av}}(t)||^2 \leq \beta_1||w_x(t)||^2 + \beta_2||w_t(t)||^2 + \beta_3|\vartheta_{\mathrm{av}}(t)|^2 \tag{81}$$

where

$$\alpha_1 = 4(1 + 4D^3||\phi'||^2) \tag{82}$$

$$\alpha_2 = 4D||n'||^2 \tag{83}$$

$$\alpha_3 = 4||\psi'||^2 \tag{84}$$

$$\beta_1 = 4||n'||^2 \tag{85}$$

$$\beta_2 = 4(1 + 4D^3||\phi||^2) \tag{86}$$

$$\beta_3 = 4||\psi KH||^2 \tag{87}$$

Applying Eq. (81), we obtain

$$\Omega(t) \leq \theta_4 \Xi(t) \tag{88}$$

where

$$\theta_4 = \max\{\alpha_1 + \beta_1, \alpha_2 + \beta_2, \alpha_3 + \beta_3\} \tag{89}$$

With the help of time and space derivatives of Eq. (28)—see Ref. [30] for more details—and applying again Poincare's, Young's, and the Cauchy-Schwartz inequalities, we obtain the following inequalities:

$$||w_x(t)||^2 \leq a_1||\partial_x u_{\mathrm{av}}(t)||^2 + a_2||\partial_t u_{\mathrm{av}}(t)||^2 + a_3|\vartheta_{\mathrm{av}}(t)|^2 \tag{90}$$

$$||w_t(t)||^2 \leq b_1||\partial_x u_{\mathrm{av}}(t)||^2 + b_2||\partial_t u_{\mathrm{av}}(t)||^2 + b_3|\vartheta_{\mathrm{av}}(t)|^2 \tag{91}$$

by means of them, we obtain

$$\theta_3 \Xi \leq \Omega(t) \tag{92}$$

where

$$\theta_3 = \frac{1}{\max\{a_1 + b_1, a_2 + b_2, a_3 + b_3 + 1\}} \tag{93}$$

With the help of Eqs. (66), (78), (88), and (92), we get

$$\Omega(t) \leq \frac{\theta_1\theta_3}{\theta_2\theta_4}\Omega(0)e^{-\eta t} \tag{94}$$

which completes the proof of exponential stability of the average closed-loop system in sense of the norm (62) in the variables $(\vartheta_{\mathrm{av}}, u_{\mathrm{av}})$.

5.5 Step 5: Invoking the Averaging Theorem for Infinite-Dimensional Systems.
The main idea is to convert the wave equation in the closed-loop system (41)–(44) to a cascade of two first-order transport equations which convect in opposite directions. To achieve this, we define the following Riemann transformations [22]:

$$\bar{\zeta}(x,t) = u_t(x,t) + u_x(x,t) \tag{95}$$

$$\bar{\omega}(x,t) = u_t(x,t) - u_x(x,t) \tag{96}$$

together with their inverses given by

$$u_t(x,t) = \frac{\bar{\zeta}(x,t) + \bar{\omega}(x,t)}{2} \qquad (97)$$

$$u_x(x,t) = \frac{\bar{\zeta}(x,t) - \bar{\omega}(x,t)}{2} \qquad (98)$$

Defining

$$\xi(t) = u(0,t) \qquad (99)$$

and noting that $\bar{\zeta}(0,t) = \dot{\xi}(t) + u_x(0,t)$, system (41)–(44) is written as

$$\dot{\vartheta}(t) = \frac{\bar{\zeta}(0,t) - \bar{\omega}(0,t)}{2} \qquad (100)$$

$$\dot{\xi}(t) = \frac{\bar{\zeta}(0,t) + \bar{\omega}(0,t)}{2} \qquad (101)$$

$$\bar{\omega}_t(x,t) = -\bar{\omega}_x(x,t) \qquad (102)$$

$$\bar{\omega}(0,t) = \bar{\zeta}(0,t) - 2u_x(0,t) \qquad (103)$$

$$\bar{\zeta}_t(x,t) = \bar{\zeta}_x(x,t) \qquad (104)$$

$$\bar{\zeta}(D,t) = U(t) + u_t(D,t) \qquad (105)$$

$$\dot{U}(t) = -cU(t) + c\left\{ \bar{c}[K\hat{H}(t)u(D,t) - u_t(D,t)] \right.$$
$$\left. + \bar{\rho}(D)KG(t) + K\hat{H}(t)\int_0^D \bar{\rho}(D - \sigma)u_t(\sigma,t)d\sigma \right\} \qquad (106)$$

In this new framework, the wave phenomenon is represented as the cascade of two transport PDEs, with two ODE (simple integrators), being driven by the two PDEs. The ODE (100) plays a central role since it was made stable by feedback, which is applied through the transport Eq. (104) at the boundary $x = D$ in this new representation form. The second ODE (101) is already at the equilibrium $\xi(t) \equiv 0$ by the choice of the boundary condition (43) and (99). A second transport phenomenon (102) is also present, in the opposite direction, accounting for the reflection of the wave at $x = 0$.

The subsystem (100) and (104)–(106) can also be interpreted as an input-delay ordinary differential equation, delayed by D units of time, followed by a stable transport phenomenon (102)–(103). Hence, the closed-loop system (100)–(106) can be rewritten as

$$\dot{z}(t) = f(\omega t, z_t) \qquad (107)$$

where $z(t) = [\tilde{\vartheta}(t), \xi(t), U(t)]^T$ is the state vector and the distributed terms are encompassed by $z_t(r) = z(t + r)$ for $-D \leq r \leq 0$, with f being an appropriate continuous functional, such that the averaging theorem by Hale and Lunel [26] (Sec. 5) can be directly applied, considering $\omega = 1/\epsilon$.

Since we have already proved the origin of the average closed-loop system with wave PDE is exponentially stable according to Eq. (94) and $\xi_{av}(t) \equiv 0$ from Eqs. (43) and (99), by applying the averaging theorem for infinite-dimensional systems developed in Sec. 5 of Ref. [26], for ω sufficiently large, we conclude (49)–(52) has an unique exponentially stable periodic solution around its equilibrium satisfying (45).

5.6 Step 6: Convergence to a Neighborhood of the Extremum Point $(\theta^*, \Theta^*, y^*)$**.** Applying Agmon's, Poincare's and Young's inequality on the left-hand side of Eq. (9), along with Eqs. (9)–(12), we have

$$\tilde{\theta}^2(t) \leq (1 + 2D)\vartheta(t)^2 + (4D^2 + 1)||\bar{\alpha}_x(t)||^2 \qquad (108)$$

Using the again the Poincare inequality

$$||\bar{\alpha}_x(t)||^2 \leq 2\bar{\alpha}_x(0,t)^2 + 4D^2||\bar{\alpha}_{xx}(t)||^2 \qquad (109)$$

with $\bar{\alpha}_x(0,t) = \vartheta(t)$ from Eq. (9) and $\partial_t u(x,t) = \partial_{tt}\bar{\alpha}(x,t) = \partial_{xx}\bar{\alpha}(x,t)$ from Eqs. (10) and (18), we can rewrite Eq. (108) as

$$\tilde{\theta}^2(t) \leq (3 + 2D + 8D^2)\vartheta(t)^2 + (16D^4 + 4D^2)||\partial_t u(t)||^2 \qquad (110)$$

Inequality (110) can be written in terms of the periodic solution $\vartheta^\Pi(t)$ and $\partial_t u^\Pi(x,t)$ as follows:

$$\limsup_{t\to\infty} |\tilde{\theta}(t)|^2$$
$$= \limsup_{t\to\infty}\{(3 + 2D + 8D^2)|\vartheta(t) + \vartheta^\Pi(t) - \vartheta^\Pi(t)|^2\}$$
$$+ \limsup_{t\to\infty}\{(16D^4 + 4D^2)||\partial_t u(t) + \partial_t u^\Pi(t) - \partial_t u^\Pi(t)||^2\} \qquad (111)$$

By applying Young's inequality and some algebra it holds

$$|\vartheta(t) + \vartheta^\Pi(t) - \vartheta^\Pi(t)|^2 \leq \sqrt{2}(|\vartheta(t) - \vartheta^\Pi(t)|^2 + |\vartheta^\Pi(t)|^2)$$

The same procedure can be applied to the second term on the right-hand side of Eq. (111). From the averaging theorem [26], we know that $\vartheta(t) - \vartheta^\Pi(t) \to 0$ and $\partial_t u(t) - \partial_t u^\Pi(t) \to 0$, exponentially as $t \to +\infty$. Hence

$$\limsup_{t\to\infty} |\tilde{\theta}(t)|^2 = \limsup_{t\to\infty}\{\sqrt{2}(3 + 2D + 8D^2)|\vartheta^\Pi(t)|^2\}$$
$$+ \limsup_{t\to\infty}\{\sqrt{2}(16D^4 + 4D^2)||\partial_t u^\Pi(t)||^2\} \qquad (112)$$

Along with Eq. (45), it is not difficult to show

$$\limsup_{t\to\infty} |\tilde{\theta}(t)| = \mathcal{O}(1/\omega) \qquad (113)$$

From Eq. (8) and Fig. 3, we can write $\theta(t) - \theta^* = \tilde{\theta}(t) + S(t)$, and recalling $S(t)$ in Eq. (23) is of order $\mathcal{O}(a)$, we finally get with Eq. (46). The convergence of the propagated actuator $\Theta(t)$ to the optimizer Θ^* is easier to prove. Using Eq. (24) and taking its absolute value, one has

$$|\Theta(t) - \Theta^*| = |\vartheta(t) + a\sin(\omega(t))| \qquad (114)$$

As in the convergence proof of the parameter $\theta(t)$ to the optimal input θ^* above, we write Eq. (114) in terms of the periodic solution $\vartheta^\Pi(t)$ and follow the same steps by applying Young's inequality and reminding that $\vartheta(t) - \vartheta^\Pi(t) \to 0$ exponentially according to the averaging theorem [26]. Hence, along with Eq. (45), we finally get Eq. (47). To show the convergence of the output $y(t)$ of the static map to the optimal value y^*, we replace $\Theta(t) - \Theta^*$ in Eq. (7) by Eq. (24) and take the absolute value

$$|y(t) - y^*| = \left| \frac{H}{2}[\vartheta(t) + a\sin(\omega(t))]^2 \right| \qquad (115)$$

Expanding the quadratic term in Eq. (115) and applying Young's inequality to the resulted equation, one has $|y(t) - y^*| = |H[\vartheta(t)^2 + a^2 \sin^2(\omega t)]|$. As before, we add and subtract the periodic solution $\vartheta^\Pi(t)$ and use the convergence of $\vartheta(t) - \vartheta^\Pi(t) \to 0$ via averaging theorem [26]. Hence, again with Eq. (45), we get Eq. (48). ∎

In the next sections, alternative extremum seeking schemes for wave PDE compensation are presented using different actuation

topology (Dirichlet rather than Neumann)—Sec. 6—as well as feedback loops and cascades with wave PDEs—Sec. 7.

6 Extremum Seeking for Wave Partial Differential Equations With Dirichlet Actuation

We now return to the problem formulation as in Sec. 3.2, but with a distinct choice for the actuated variable in the wave PDE.

For the sake of clarity, in what follows we set $c \to +\infty$ so that we can focus our attention on the design of the new feedback controller and do not distract the readers with technical details of including the low-pass filter in the closed-loop, as done in Eq. (40). However, as discussed in Ref. [6], it is worth mention that the inclusion of the filter $c/(s+c)$ is a fundamental step which allows us to apply the average theorem for infinite-dimensional systems [26] and complete the proof of our theorems.

In this sense, we consider the system

$$\Theta(t) = \alpha(0,t) \tag{116}$$

$$\partial_{tt}\alpha(x,t) = \partial_{xx}\alpha(x,t), \quad x \in [0,D] \tag{117}$$

$$\partial_x\alpha(0,t) = 0 \tag{118}$$

$$\alpha(D,t) = \theta(t) \tag{119}$$

where instead of the Neumann actuation choice, $\partial_x\alpha(D,t) = \theta(t)$, we consider Dirichlet actuation, $\alpha(D,t) = \theta(t)$.

In the Dirichlet case, Eqs. (14)–(17) can be rewritten as

$$\dot{\vartheta}(t) = u(0,t) \tag{120}$$

$$\partial_{tt}u(x,t) = \partial_{xx}u(x,t), \quad x \in [0,D] \tag{121}$$

$$\partial_x u(0,t) = 0 \tag{122}$$

$$u(D,t) = U(t) \tag{123}$$

The control law is obtained as in chapter 16.4 of [32]

$$U(t) = c_0 K \hat{H}(t) \int_0^D (1 + M(D-y))u(y,t)dy$$
$$+ K\hat{H}(t)\int_0^D m(D-y)u_t(y,t)dy - c_0\int_0^D u_t(y,t)dy$$
$$+ KM(D)G(t) \tag{124}$$

where $\hat{H}(t)$ and $G(t)$ are the same signals given by Eqs. (26) and (27), respectively. Moreover, the functions $M(\cdot)$ and $m(\cdot)$ are simply

$$M(s) = [I\ 0]e^{As}[I\ 0]^T, \quad A = \begin{pmatrix} 0 & 0 \\ I & 0 \end{pmatrix} \tag{125}$$

$$m(s) = \int_0^s M(\xi)d\xi \tag{126}$$

On the other hand, the signal $S(t)$ in Eqs. (19)–(22) must be redesigned according to the trajectory generation problem described in chapter 12 of [25] for Dirichlet actuation, leading us to

$$S(t) = \frac{a}{2}\left[\sin(\omega(t+D)) + \sin(\omega(t-D))\right] \tag{127}$$

Notice that the trajectory generation problem for the wave PDE with Dirichlet actuation is a particular case of the wave equation with Kelvin–Voigt damping $(\epsilon\partial_{tt}u(x,t) = (1 + d\partial_t)\partial_{xx}u(x,t)$, $\partial_x u(0,t) = 0$, $\epsilon, d > 0)$, studied in Ref. [17].

Thus, the resulting average target system for the wave equation with Dirichlet actuation becomes

$$\dot{\vartheta}_{av}(t) = KH\vartheta_{av}(t) + w(0,t) \tag{128}$$

$$\partial_{tt}w(x,t) = \partial_{xx}w(x,t), \quad x \in [0,D] \tag{129}$$

$$\partial_x w(0,t) = c_0\partial_t w(0,t), \quad c_0 > 0 \tag{130}$$

$$w(D,t) = 0 \tag{131}$$

which is exponentially stable with the following spectrum (decay rate):

$$\mathrm{eig}\{KH\} \cup \left\{ -\frac{1}{2}\ln\left|\frac{1+c_0}{1-c_0}\right| + j\frac{\pi}{D}\left\{ \begin{matrix} n+\frac{1}{2}, & 0 \le c_0 < 1 \\ n, & c_0 > 1 \end{matrix} \right\} \right\} \tag{132}$$

The fact that we employ Dirichlet actuation at $x = D$ prevent us from applying damping at this end; hence, we induce boundary damping at the opposite end.

Although we do not have space here to detail the analysis, a similar stability theorem can be proved as for the case of Neumann actuation in Theorem 1.

Remark 1. The control law (124) can be expressed in terms of $U(t)$ rather than $u(x,t)$, according to the chapter 16.5 of Ref. [32]

$$U(t) = \frac{1}{1+c_0\tanh(Ds)}\left[KM(D)G(t)\right]$$
$$+ \frac{1}{1+e^{-2s}+c_0(1-e^{-2Ds})}\left[K\hat{H}(t)\mathcal{D}(t)\right] \tag{133}$$

where

$$\mathcal{D}(t) = \int_{t-D}^t \rho(t-\tau)U(\tau)d\tau - \int_{t-2D}^{t-D}\rho(\tau-t+2D)U(\tau)d\tau \tag{134}$$

with $\rho(\tau) = c_0 + (1+c_0)M(\tau)$.

7 Extremum Seeking for Cascades of Partial Differential Equations and Feedback Loops

In this section, we deal with distinct feedback loops and cascades of hyperbolic PDEs with wave equations. We cope with: (a) an antistable wave PDE described as two coupled transport (delay) equations and (b) an antistable wave PDE with input delay (hyperbolic transport equation).

Due to space constraints, our presentation is restricted again to derive the extremum seeking feedback laws $U(t)$, obtain the additive dither $S(t)$ which solves the trajectory generation problem formulated in chapter 12 of [25] and make briefly statements of the closed-loop properties. Unlike the developments of Sec. 5, we forgo a detailed Lyapunov stability analysis and the associated estimates for the transformations between the plant and the target systems.

7.1 Antistable Wave Partial Differential Equation as a Feedback Loop of Two Transport (Delay) Partial Differential Equations.
In this section, we consider wave PDEs with boundary antidamping:

$$\Theta(t) = \alpha(0,t) \tag{135}$$

$$\partial_{tt}\alpha(x,t) = \partial_{xx}\alpha(x,t), \quad x \in [0,D] \tag{136}$$

$$\partial_x\alpha(0,t) = -q\partial_t\alpha(0,t), \quad |q| \neq 1 \tag{137}$$

$$\partial_x\alpha(D,t) = \theta(t) \tag{138}$$

where θ is the input appearing in the form of Neumann actuation and the output Θ as a Dirichlet sensor. The damping coefficient $q \geq 0$ is considered to be known. As discussed in chapter 19 of Ref. [32], when $q = 1$, the real part of the plant (infinite) eigenvalues is $+\infty$ while, for $q \neq 1$ and $q \geq 0$, the real part is positive but finite. Consequently, we can rewrite Eqs. (9)–(12) into

$$\vartheta(t) := \bar{\alpha}(0,t) \qquad (139)$$

$$\partial_{tt}\bar{\alpha}(x,t) = \partial_{xx}\bar{\alpha}(x,t), \quad x \in [0,D] \qquad (140)$$

$$\partial_x\bar{\alpha}(0,t) = -q\partial_t\bar{\alpha}(0,t), \quad |q| \neq 1 \qquad (141)$$

$$\partial_x\bar{\alpha}(D,t) = \tilde{\theta}(t) \qquad (142)$$

and, reminding that $u(x,t) = \partial_t\bar{\alpha}(x,t)$, Eqs. (14)–(17) such as

$$\dot{\vartheta}(t) = u(0,t) \qquad (143)$$

$$\partial_{tt}u(x,t) = \partial_{xx}u(x,t), \quad x \in [0,D] \qquad (144)$$

$$\partial_x u(0,t) = -q\partial_t u(0,t), \quad |q| \neq 1 \qquad (145)$$

$$\partial_x u(D,t) = U(t) \qquad (146)$$

Analogous to the developments carried out in Step 5 for the proof of Theorem 1, we use again the Riemann-like transformations [22] but now for the system (135)–(138) such that we can redefine

$$\bar{\zeta}(x,t) = \frac{1}{1-q}[u_t(x,t) + u_x(x,t)] \qquad (147)$$

$$\bar{\omega}(x,t) = \frac{1}{1+q}[u_t(x,t) - u_x(x,t)] \qquad (148)$$

with their corresponding inverses given by

$$u_t(x,t) = \frac{(1-q)\bar{\zeta}(x,t) + (1+q)\bar{\omega}(x,t)}{2} \qquad (149)$$

$$u_x(x,t) = \frac{(1-q)\bar{\zeta}(x,t) - (1+q)\bar{\omega}(x,t)}{2} \qquad (150)$$

Hence, Eqs. (143)–(146) is reshaped as

$$\text{ODE:} \quad \dot{\vartheta}(t) = \bar{\zeta}(0,t) \qquad (151)$$

$$\text{PDE 1:} \begin{cases} \bar{\zeta}_t(x,t) = \bar{\zeta}_x(x,t), \quad x \in [0,D] \\ \bar{\zeta}(D,t) = \frac{1}{1-q}[U(t) + u_t(D,t)] \end{cases} \qquad (152)$$

$$\text{PDE 2:} \begin{cases} \bar{\omega}_t(x,t) = -\bar{\omega}_x(x,t), \quad x \in [0,D] \\ \bar{\omega}(0,t) = \bar{\zeta}(0,t) \end{cases} \qquad (153)$$

Applying the back-stepping transformations [22]

$$w(x,t) = \bar{\zeta}(x,t) - KH\int_0^x \bar{\zeta}(\sigma,t)d\sigma - KH\vartheta(t) \qquad (154)$$

$$\varpi(x,t) = \bar{\omega}(x,t) + KH\int_0^x \bar{\omega}(\sigma,t)d\sigma - KH\vartheta(t) \qquad (155)$$

the resulting average target system for Eqs. (151)–(153) is

$$\dot{\vartheta}_{av}(t) = KH\vartheta_{av}(t) + w_{av}(0,t) \qquad (156)$$

$$\partial_t w_{av}(x,t) = \partial_x w_{av}(x,t), \quad w_{av}(0,t) = \varpi_{av}(0,t) \qquad (157)$$

$$\partial_t \varpi_{av}(x,t) = -\partial_x \varpi_{av}(x,t) \qquad (158)$$

$$w_{av}(D,t) = -\frac{1}{c}\partial_t\partial_x u_{av}(D,t) \qquad (159)$$

which is exponentially stable for $c > 0$ sufficiently large. This result is not difficult of proving since (156) is exponentially ISS [29] with respect to $w_{av}(0,t)$. On the other hand, $w_{av}(x,t)$ is finite-time stable with respect to $\varpi_{av}(0,t)$ and $\varpi_{av}(x,t)$ is asymptotically stable for $c \to +\infty$ (or $w_{av}(D,t) \to 0$) [22].

Plugging (154) with $x = D$ into (159), we can write $\dot{U}_{av}(t) = -cw_{av}(D,t)$ according to Eq. (146) as

$$\dot{U}_{av}(t) = -c\bar{\zeta}_{av}(D,t) + cK\left[H\vartheta_{av}(t) + H\int_0^D \bar{\zeta}_{av}(x,t)dx\right] \qquad (160)$$

Plugging the average version of Eqs. (152) and (147) into Eq. (160), one has

$$\dot{U}_{av}(t) = -\frac{c}{1-q}[U_{av}(t) + \partial_t u_{av}(D,t)]$$
$$+ cK\left[H\vartheta_{av}(t) + H\int_0^D \frac{1}{1-q}[\partial_t u_{av}(x,t) + \partial_x u_{av}(x,t)]dx\right] \qquad (161)$$

which can be rewritten as

$$\dot{U}_{av}(t) = -\bar{c}U_{av}(t) - \bar{c}\partial_t u_{av}(D,t)$$
$$+ \bar{c}K\left[(1-q)H\vartheta_{av}(t) + H\int_0^D [\partial_t u_{av}(x,t) + \partial_x u_{av}(x,t)]dx\right] \qquad (162)$$

or, equivalently

$$U_{av}(t) = \frac{\bar{c}}{s+\bar{c}}\left\{-\partial_t u_{av}(D,t) + K\left[(1-q)H\vartheta_{av}(t)\right.\right.$$
$$\left.\left. + H\int_0^D [\partial_t u_{av}(x,t) + \partial_x u_{av}(x,t)]dx\right]\right\} \qquad (163)$$

where $\bar{c} = c/(1-q)$. Reminding that $G_{av}(t) = H\vartheta_{av}(t)$ and $\hat{H}_{av}(t) = H$ from Eq. (36), one can finally obtain the implementable control law

$$U(t) = \frac{\bar{c}}{s+\bar{c}}\left\{-u_t(D,t)\right.$$
$$\left. + K\left[(1-q)G(t) + \hat{H}(t)\int_0^D [u_t(x,t) + u_x(x,t)]dx\right]\right\} \qquad (164)$$

with $\hat{H}(t)$ and $G(t)$ defined by Eqs. (26) and (27), respectively.

The last stage is to obtain the additive dither $S(t)$ solving the following trajectory generation problem:

$$S(t) := \partial_x\beta(D,t) \qquad (165)$$

$$\partial_{tt}\beta(x,t) = \partial_{xx}\beta(x,t), \quad x \in [0,D] \qquad (166)$$

$$\partial_x\beta(0,t) = -q\partial_t\beta(0,t), \quad |q| \neq 1 \qquad (167)$$

$$\beta(0,t) = a\sin(\omega t) \qquad (168)$$

The explicit solution of Eq. (165) is given according to chapter 12 of Ref. [25]

$$S(t) = -a\omega\sin(\omega D)\cos(\omega t) - aq\omega\cos(\omega D)\cos(\omega t) \qquad (169)$$

since $\beta(x,t) = a\cos(\omega x)\sin(\omega t) - aq\sin(\omega x)\cos(\omega t)$.

Remark 2. A similar result can be provided for the Dirichlet actuation $\alpha(D,t) = \theta(t)$, $\bar{\alpha}(D,t) = \tilde{\theta}(t)$ and $u(D,t) = U(t)$ by redefining the Riemann transformations (147) and (148) to

$$\bar{\zeta}(x,t) = \frac{1}{1-q}[\bar{\alpha}_t(x,t) + \bar{\alpha}_x(x,t)] \tag{170}$$

$$\bar{\omega}(x,t) = \frac{1}{1+q}[\bar{\alpha}_t(x,t) - \bar{\alpha}_x(x,t)] \tag{171}$$

In this case, the control law can be expressed in terms of $\bar{\alpha}(x,t)$ rather than $u(x,t)$, according to

$$U(t) = \frac{\bar{c}}{s+\bar{c}}\left\{-\partial_x\bar{\alpha}(D,t) + K\left[(1-q)G(t) + \hat{H}(t)\right.\right.$$
$$\left.\left. \times \int_0^D [u(x,t) + \partial_x\bar{\alpha}(x,t)]dx\right]\right\} \tag{172}$$

with $\hat{H}(t)$ and $G(t)$ defined by Eqs. (27) and (26), respectively. Reminding Eq. (25), the control law (172) is indeed implementable since $\partial_x\bar{\alpha}(x,t)$ can be written in terms of measurable signals

$$\partial_x\bar{\alpha}(x,t) = \partial_x\alpha(x,t) - \partial_x\beta(x,t) \tag{173}$$

and the integral in Eq. (172) is given by

$$\int_0^D \partial_x\bar{\alpha}(x,t)dx = \bar{\alpha}(D,t) - \bar{\alpha}(0,t)$$
$$= \alpha(D,t) - \beta(D,t) - \Theta^* - \alpha(0,t) + \beta(0,t) + \Theta^*$$
$$= \theta(t) - \beta(D,t) - \Theta(t) + a\sin(\omega t) \tag{174}$$

The term $\beta(x,t)$ is defined like the trajectory generation problem (165)–(168) but replacing (165) by $S(t) := \beta(D,t)$, which leads to [25] (chapter 12):

$$S(t) = a\cos(\omega D)\sin(\omega t) - aq\sin(\omega D)\cos(\omega t) \tag{175}$$

since $\beta(x,t) = a\cos(\omega x)\sin(\omega t) - aq\sin(\omega x)\cos(\omega t)$. Notice that (175) exactly matches (after some manipulations) to Eq. (127) when $q = 0$ is set in Eq. (175).

7.2 Antistable Wave Partial Differential Equation With Input Delay. Inspired by reference [12], we discuss the extension of our ES approach for the same antistable wave PDE of the previous section but now with a delayed input. This is particularly an important problem since Datko et al. [33] showed that standard feedback laws for wave equations have a zero robustness margin to the introduction of a delay in the feedback loop.

Hence, we consider the delay-wave cascade system

$$\Theta(t) = \alpha(0,t) \tag{176}$$

$$\partial_{tt}\alpha(x,t) = \partial_{xx}\alpha(x,t), \quad x \in [0,1] \tag{177}$$

$$\partial_x\alpha(0,t) = -q\partial_t\alpha(0,t), \quad |q| \neq 1 \tag{178}$$

$$\alpha(1,t) = \theta(t-D) \tag{179}$$

where $\alpha(x,t)$ is the infinite-dimensional state of the antistable wave PDE with spatial domain defined without loss of generality by $x \in [0,1]$. The boundary delay is denoted by $D > 0$ being any arbitrary known constant.

The delay-wave system is alternatively written as [12]

$$\dot{\vartheta}(t) = u(0,t) \tag{180}$$

$$\partial_{tt}u(x,t) = \partial_{xx}u(x,t), \quad x \in [0,1] \tag{181}$$

$$\partial_x u(0,t) = -q\partial_t u(0,t), \quad |q| \neq 1 \tag{182}$$

$$u(1,t) = v(1,t) \tag{183}$$

$$\partial_t v(x,t) = \partial_x v(x,t), \quad x \in [1,1+D] \tag{184}$$

$$v(1+D,t) = U(t) \tag{185}$$

where $U(t)$ is the overall system (control) input and (ϑ,u,v) is the state of the ODE–PDE–PDE cascade. From the transport PDE representation form for the input delay, we know that [32] (chapter 2):

$$v(x,t) = U(t+x-1-D), \quad x \in [1,1+D] \tag{186}$$

Reminding that Eqs. (181)–(183) can be represented into Eqs. (152)–(153), applying the transformations

$$w(x,t) = \bar{\zeta}(x,t) - KH\int_0^x \bar{\zeta}(\sigma,t)d\sigma - KH\vartheta(t), \quad x \in [0,1] \tag{187}$$

$$\varpi(x,t) = \bar{\omega}(x,t) + KH\int_0^x \bar{\omega}(\sigma,t)d\sigma - KH\vartheta(t), \quad x \in [0,1] \tag{188}$$

$$\zeta(x,t) = v(x,t) - KH\int_1^x v(\sigma,t)d\sigma$$
$$+ \frac{1}{1-q}\bar{\alpha}_x(1,t) - KH\int_0^1 \bar{\zeta}(\sigma,t)d\sigma - KH\vartheta(t), \quad x \in [1,1+D] \tag{189}$$

the resulting average target system for Eqs. (180)–(185) is

$$\dot{\vartheta}_{\mathrm{av}}(t) = KH\vartheta_{\mathrm{av}}(t) + w_{\mathrm{av}}(0,t) \tag{190}$$

$$\partial_t w_{\mathrm{av}}(x,t) = \partial_x w_{\mathrm{av}}(x,t), \quad w_{\mathrm{av}}(0,t) = \varpi_{\mathrm{av}}(0,t) \tag{191}$$

$$\partial_t \varpi_{\mathrm{av}}(x,t) = -\partial_x \varpi_{\mathrm{av}}(x,t) \tag{192}$$

$$w_{\mathrm{av}}(1,t) = \zeta_{\mathrm{av}}(1,t) \tag{193}$$

$$\partial_t \zeta_{\mathrm{av}}(x,t) = \partial_x \zeta_{\mathrm{av}}(x,t), \quad x \in [1,1+D] \tag{194}$$

$$\zeta_{\mathrm{av}}(1+D,t) = -\frac{1}{c}\partial_t v_{\mathrm{av}}(1+D,t) \tag{195}$$

From Eqs. (189) and (195), one can obtain the expression for $\dot{U}_{\mathrm{av}}(t) = -c\zeta_{\mathrm{av}}(1+D,t)$ such that

$$\dot{U}_{\mathrm{av}}(t) = -cv_{\mathrm{av}}(1+D,t) + cKH\int_1^{1+D} v_{\mathrm{av}}(\sigma,t)d\sigma$$
$$- \frac{c}{1-q}\bar{\alpha}_x(1,t) + cKH\int_0^1 \bar{\zeta}_{\mathrm{av}}(\sigma,t)d\sigma + cKH\vartheta_{\mathrm{av}}(t) \tag{196}$$

Plugging Eq. (186) into Eq. (196), we can obtain the control law

$$U(t) = \frac{c}{s+c}\left\{\frac{-1}{1-q}\bar{\alpha}_x(1,t) + K\left[G(t) + \hat{H}(t)\int_{t-D}^t U(\tau)d\tau\right.\right.$$
$$\left.\left. + \hat{H}(t)\int_0^1 \frac{1}{1-q}[u(x,t) + \bar{\alpha}_x(x,t)]dx\right]\right\} \tag{197}$$

for $c > 0$ sufficiently large, $u(x,t) = \bar{\alpha}_t(x,t)$ and $\bar{\alpha}_x(x,t)$ satisfying (173)–(174).

As discussed in Ref. [6], the explicit solution of the trajectory generation problem [25] (chapter 12) under delays would be solved from (175) as $S(t - D) = a\cos(\omega D)\sin(\omega t) - aq\sin(\omega D)\cos(\omega t)$, leading us to

$$S(t) = a\cos(\omega D)\sin(\omega(t+D)) - aq\sin(\omega D)\cos(\omega(t+D))$$

(198)

8 Numerical Simulations

The academic example studied in this section can be faced as a very simplified version of the drilling control problem described in Sec. 2. No particular modeling of specific nonlinear phenomena for the oil drilling problem was taken into account in this section. However, pairing this real-time optimal drilling problem and the proposed PDE-based extremum seeking methods sounds promising. It seems we can improve performance by compensating the PDE-drill dynamics into the extremum-seeking loop. We can assume the drill model as a string of delay dynamics or simply a wave PDE, as discussed in reference [23].

One issue is that in practice we would ideally like to model the downhole boundary as an ODE, coupled with the PDE. We do not think this is required to come up with a worthwhile result, but it would be nice if this is something we are able to handle. We have not studied the compensation of wave PDEs in the presence of ODE dynamics but we do not see why this would not be doable. We just need to assume that the ODE is "fast", namely, we have to use the frequency ω (of the signals $S(t)$, $M(t)$, and $N(t)$) that is slower than the ODE's time constants, and then have to estimate the gradient/derivative of the map in the steady-state (as a static map of Assumption 1). This would roughly mirror what is done with the singular perturbation approach in the paper [1] for ES oriented to nonlinear ODE-dynamics.

There may be an obstacle to getting a theorem because we may not have a singular perturbation that we need for systems with delays and/or wave PDEs. But, in light of this attractive application, it would be worth considering the study for future research. And, insofar as simply using the algorithm is concerned, which may be practitioners primary concern, this should be simple— as said above, ω and the "dither" signals $\sin(\omega t)$ just have to be chosen slow compared to the ODE dynamics. Basically, when non-compensated dynamics are present such perturbation signals used in extremum seeking need to be slow. In this case, we prefer to call it "slither" (the slow wiggly gait of a snake). Also, slither- = sl(ow-d)ither.

Here, for the sake of simplicity we just consider the wave PDE dynamics in cascade with the static map as described in (1)–(6) and illustrated in Fig. 1. No other unmodeled dynamics is addressed such that the dither signals can still be chosen with a sufficiently large frequency. Due to space constraints, we will focus on showing the numerical simulations only for the extremum seeking feedback for antistable wave PDEs with Dirichlet boundary actuation of Sec. 7.1 (Remark 2).

In this context, we consider a quadratic static map as in Eq. (6), with Hessian $H = -2$, optimizer $\Theta^* = \theta^* = 2$, and optimal value $y^* = 5$. The domain length of the wave PDE and the damping coefficient were set to $D = 1$ and $q = 5$, respectively. The parameters of the proposed ES are chosen as $\omega = 10$, $a = 0.2$, $c = 10$, $\bar{c} = 0.5$, and $K = 0.2$.

The corresponding numerical plots of the closed-loop system are given in Figs. 4(a) and 4(b). We note that the signals Θ and θ converge to a close neighborhood of the optimizer $\Theta^* = \theta^*$.

Figures 5(a) and 5(b) present relevant variables for ES. It is clear that the remarkable evolution of the output signal $y(t)$ and the Hessian's estimate $\hat{H}(t)$ ultimately achieving the extremum $y^* = 5$ and the correct Hessian value $H = -2$, even in the presence of the wave PDE.

Remark 3. Persistent perturbations are a necessity if the algorithm were to remain alert to changes in the system [34]. The persistence of oscillation allows to re-optimize the operation as equipment ages, the drill bit wears, and passes from one rock type to another. In practice, high-frequency oscillations in the plots of Figs. 4(a) and 4(b) due to the persistent excitation signal S(t) may also lead to chattering or limit cycles in actuators. The inability to remove it and achieve equilibrium stabilization in ES may also be associated with actuator constraints, such as magnitude and rate saturation. Here, the best control requirement could be to enforce a stable, "smallest" limit cycle [35] (chapter 5). However, ES-based controllers whose control efforts vanish as the system approaches equilibrium have been proposed [36,37]. In Refs. [3] and [38–40], Lie bracket-based ES was also introduced to obtain feedback controllers with bounded update rates. Hence, limit cycles may not only be reduced, but they can also be completely eliminated in these cases.

In Figs. 6(a) and 6(b), the proposed ES scheme with PDE compensation is compared to the classical ES design [1]. Using the same parameters for ω, a, and K of the prior simulation, results in instability of $\theta(t)$ and $\Theta(t)$, as illustrated in Fig. 6(a). On the other hand, Fig. 6(b) shows the response for a lower frequency $\omega = 0.4$ rad/s, in which we observe that the stability can be recovered but the convergence speed gets much slower (around 30 times!) than
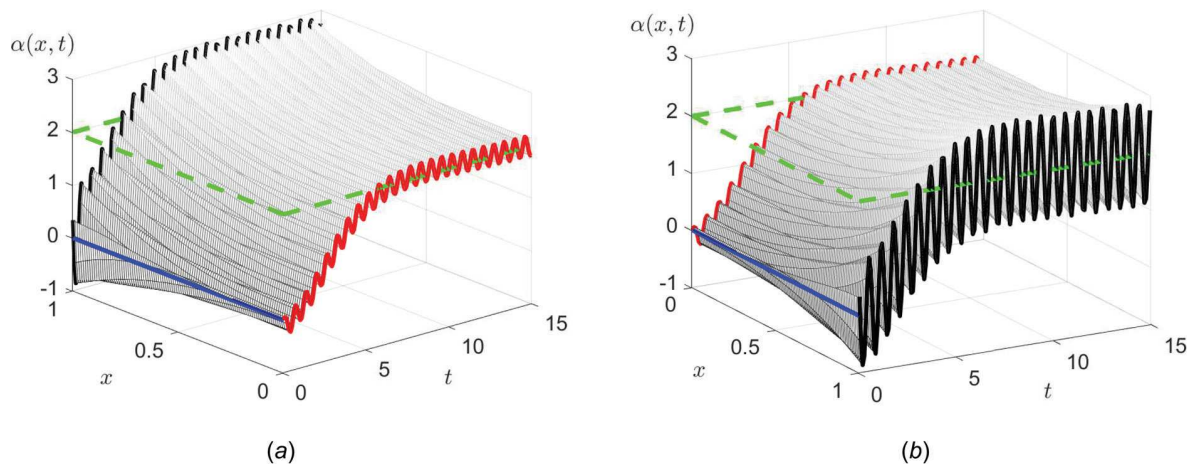

(a)   (b)

Fig. 4 Compensation of antistable wave PDEs in actuator dynamics for extremum seeking feedback with boundary Dirichlet actuation: $\alpha(0,t) = \Theta(t)$ and $\alpha(D,t) = \theta(t)$, with $D = 1$, $q = 5$, and $\Theta^* = \theta^* = 2$. (a) parameter $\Theta(t)$ (red) converging to Θ^* (dashed-green) and (b) parameter $\theta(t)$ (black) converging to θ^* (dashed-green).
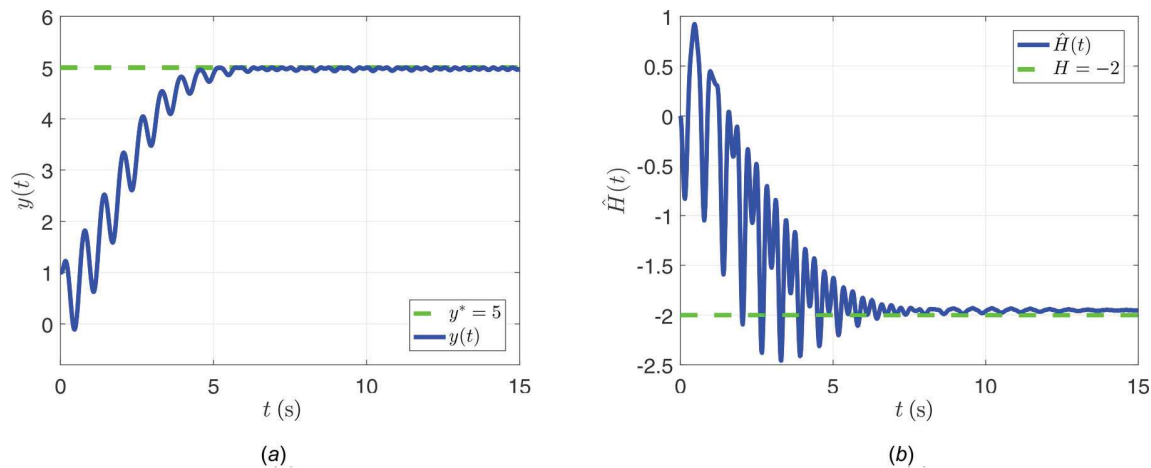
Fig. 5 Compensation of antistable wave PDEs in actuator dynamics for extremum seeking feedback with boundary Dirichlet actuation: time response of $y(t)$ converging to the extremum $y^* = 5$ and the Hessian's estimate $\hat{H}(t)$ converging to $H = -2$. (a) Output static map $y(t)$ and (b) Hessian estimate $\hat{H}(t)$.
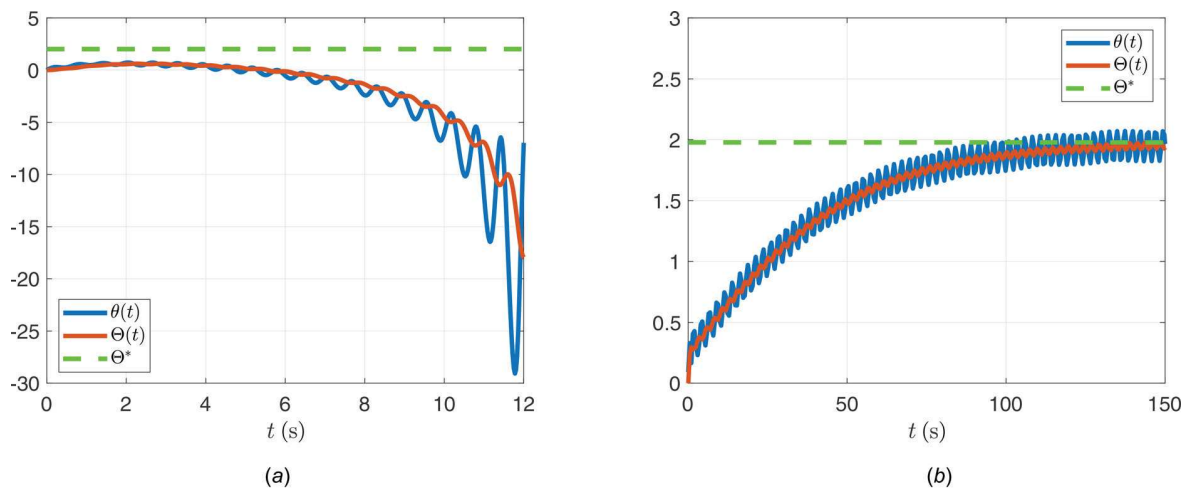

Fig. 6 Classical ES with uncompensated wave PDE actuator dynamics: (a) instability for large ω; (b) very slow convergence for small ω. (a) time evolution of the signals $\theta(t)$ and $\Theta(t)$ for large ω and (b) time evolution of the signals $\theta(t)$ and $\Theta(t)$ for small ω.
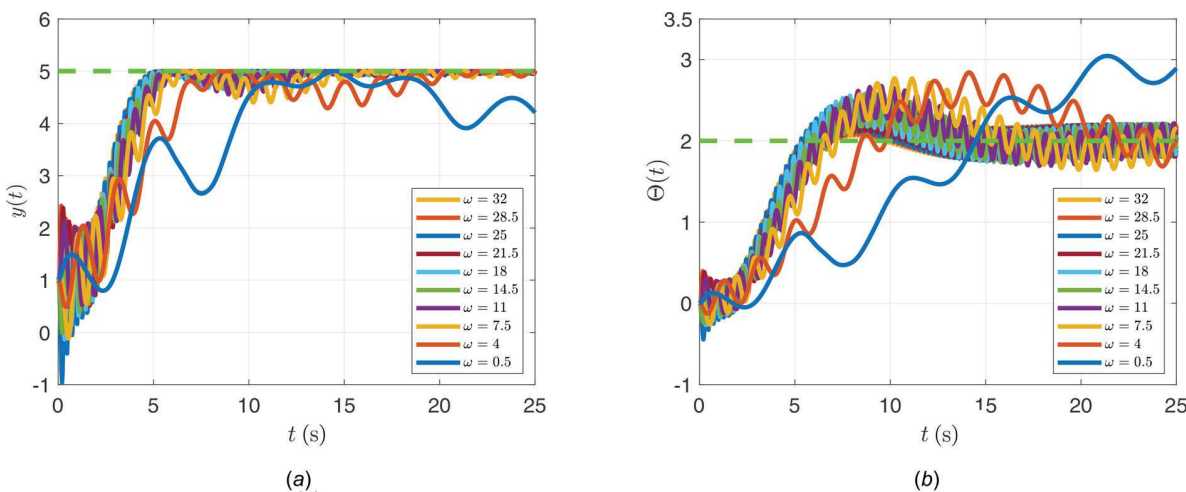

Fig. 7 Time evolution of the signals $y(t)$ and $\Theta(t)$ converging to a neighborhood of the extremum point $y^* = 5$ and the maximizer $\Theta^* = 2$ under different values of the dither frequency $\omega \in [0.006, 30]$ rad/s: (a) time evolution of the signal $y(t)$ for different values of ω and (b) time evolution of the signal $\Theta(t)$ for different values of ω

the results in Figs. 4(a) and 4(b). Hence, our proposed ES controller stands as a strong improvement of the classical ES in the presence of actuation dynamics governed by wave PDEs.

Finally, Figs. 7(a) and 7(b) present the effect of the dither frequency ω in the convergence of the algorithm for different values of $\omega \in [0.006, 30]$ rad/s. As $\omega \to 0.006$, the control system performance is severely affected, as expected, resulting in a slower convergence of the ES algorithm to the desired values. For instance, with $\omega = 0.5$ rad/s, the convergence is indeed settled down after 60 s (not show). Despite of that, the algorithm continues the search for the extremum point.

Similar tests can be performed for the design parameters K and a (curves not shown). Basically, by increasing the adaptation gain K we can accelerate the closed-loop responses, whereas by decreasing the constant a we can reduce the amplitude of the residual oscillations, according to Eqs. (46)–(48). Remind that the ultimate residual set for the error $\theta(t) - \theta^*$ in Eq. (46) is of order $\mathcal{O}(a + aq + 1/\omega)$ for the antistable wave PDE, also depending on the damping coefficient q due to the amplitude of the dither $S(t)$ defined in Eq. (175).

9 Conclusions

This paper provided a complete analysis of the gradient-based extremum seeking feedback for wave compensation in different design scenarios, including Neumann–Dirichlet actuation forms, antistable wave PDEs and delay-wave PDE cascades. The wave PDE dynamics must be known, whereas no knowledge is required for the map, that is, the parameters of the map were assumed to be unknown. The control law proposed in order to counteract the wave actuator dynamics was designed via back-stepping methodology by combining state-of-the-art techniques in the field of PDE boundary control and averaging-based estimates of the map's gradient and Hessian. The additive perturbation-dither signal was designed in order to compensate the effects of the wave dynamics as well. Local stability and ultimate convergence to a small neighborhood of the unknown extremum point were proved. Although we just have considered the gradient-based method, the proposed strategy can be directly generalized to the Newton-based extremum seeking [31] following the procedure presented in Ref. [6]. The multivariable extension of the proposed algorithm can also be achieved according to Ref. [41].

For future works, the authors expect continued efforts in data validation and experiments to demonstrate the capability of the proposed extremum seeking methodology in resolving some specific real-time optimization problems in oil drilling scenarios [23].

Nomenclature

ES = extremum seeking
ODE = ordinary differential equation
PDE = partial differential equation
ISS = input-to-state stability

References

[1] Krstić, M., and Wang, H.-H., 2000, "Stability of Extremum Seeking Feedback for General Nonlinear Dynamic Systems," Automatica, 36(4), pp. 595–601.
[2] Ghods, N., and Krstic, M., 2011, "Source Seeking With Very Slow or Drifting Sensors," ASME J. Dyn. Syst., Meas., Control, 133(4), p. 044504.
[3] Scheinker, A., and Krstic, M., 2014, "Non-C² Lie Bracket Averaging for Non-smooth Extremum Seekers," ASME J. Dyn. Syst., Meas., Control, 136(1), p. 011010.
[4] Frihauf, P., Liu, S. J., and Krstic, M., 2014, "A Single Forward-Velocity Control Signal for Stochastic Source Seeking With Multiple Nonholonomic Vehicles," ASME J. Dyn. Syst., Meas., Control, 136(5), p. 051024.
[5] Bagheri, M., Krstic, M., and Naseradinmousavi, P., 2018, "Multivariable Extremum Seeking for Joint-Space Trajectory Optimization of a High-Degrees-of-Freedom Robot," ASME J. Dyn. Syst., Meas., Control, 140(11), p. 111017.
[6] Oliveira, T. R., Krstic, M., and Tsubakino, D., 2017, "Extremum Seeking for Static Maps With Delays," IEEE Trans. Automat. Control, 62(4), pp. 1911–1926.
[7] Rusiti, D., Evangelisti, G., Oliveira, T. R., Gerdts, M., and Krstic, M., 2019, "Stochastic Extremum Seeking for Dynamic Maps With Delays," IEEE Control Syst. Lett., 3(1), pp. 61–66.
[8] Feiling, J., Koga, S., Krstić, M., and Oliveira, T. R., 2018, "Gradient Extremum Seeking for Static Maps With Actuation Dynamics Governed by Diffusion PDEs," Automatica, 95(9), pp. 197–206.
[9] Oliveira, T. R., Feiling, J., Koga, S., and Krstic, M., 2018, "Scalar Newton-Based Extremum Seeking for a Class of Diffusion PDEs," IEEE Conference on Decision and Control, Miami Beach, FL, Dec. 17–19, pp. 2926–2931.
[10] Oliveira, T. R., Feiling, J., and Krstic, M., 2019, "Extremum Seeking for Maximizing Higher Derivatives of Unknown Maps in Cascade With Reaction-Advection-Diffusion PDEs," 13th IFAC Workshop on Adaptive and Learning Control Systems, Winchester, UK, Dec. 4–6, pp. 210–215.
[11] Oliveira, T. R., Feiling, J., Koga, S., and Krstic, M., 2020, "Extremum Seeking for Unknown Scalar Maps in Cascade With a Class of Parabolic Partial Differential Equations," Int. J. Adaptive Control Signal Process., pp. 1–26.
[12] Krstic, M., 2011, "Dead-Time Compensation for Wave/String PDEs," ASME J. Dyn. Syst., Meas., Control, 133(3), p. 031004.
[13] Moura, S. J., Chaturvedi, N. A., and Krstic, M., 2014, "Adaptive Partial Differential Equation Observer for Battery State-of-Charge/State-of-Health Estimation Via an Electrochemical Model," ASME J. Dyn. Syst., Meas., Control, 136(1), p. 011015.
[14] Sezgin, A., and Krstic, M., 2015, "Boundary Backstepping Control of Flow-Induced Vibrations of a Membrane at High Mach Numbers," ASME J. Dyn. Syst., Meas., Control, 137(8), p. 081003.
[15] Ghaffari, A., Moura, S., and Krstic, M., 2015, "PDE-Based Modeling, Control, and Stability Analysis of Heterogeneous Thermostatically Controlled Load Populations," ASME J. Dyn. Syst., Meas., Control, 137(10), p. 101009.
[16] Wang, J., Koga, S., Pi, Y., and Krstic, M., 2018, "Axial Vibration Suppression in a Partial Differential Equation Model of Ascending Mining Cable Elevator," ASME J. Dyn. Syst., Meas., Control, 140(11), p. 111003.
[17] Siranosian, A., Krstic, M., Smyshlyaev, A., and Bement, M., 2009, "Motion Planning and Tracking for Tip Displacement and Deflection Angle for Flexible Beams," ASME J. Dyn. Syst., Meas., Control, 131(3), p. 031009.
[18] Gu, K., and Niculescu, S. I., 2003, "Survey on Recent Results in the Stability and Control of Time-Delay Systems," ASME J. Dyn. Syst., Meas., Control, 125(2), pp. 158–165.
[19] Evesque, S., Annaswamy, A. M., Niculescu, S., and Dowling, A. P., 2003, "Adaptive Control of a Class of Time-Delay Systems," ASME J. Dyn. Syst., Meas., Control, 125(2), pp. 186–193.
[20] Olgac, N., and Sipahi, R., 2005, "The Cluster Treatment of Characteristic Roots and the Neutral Type Time-Delayed Systems," ASME J. Dyn. Syst., Meas., Control, 127(1), pp. 88–97.
[21] Olgac, N., and Sipahi, R., 2003, "Analysis of a System of Linear Delay Differential Equations," ASME J. Dyn. Syst., Meas., Control, 125(2), pp. 215–223.
[22] Bekiaris-Liberis, N., and Krstic, M., 2014, "Compensation of Wave Actuator Dynamics for Nonlinear Systems," IEEE Trans. Automat. Control, 59(6), pp. 1555–1572.
[23] Aarsnes, U. J. F., Aamo, O. M., and Krstic, M., 2019, "Extremum Seeking for Real-Time Optimal Drilling Control," American Control Conference, Philadelphia, PA, July 10–12, pp. 5222–5227.
[24] Krstić, M., 2009, "Compensating a String PDE in the Actuation or Sensing Path of an Unstable ODE," IEEE Trans. Automat. Control, 54(6), pp. 1362–1368.
[25] Krstić, M., and Smyshlyaev, A., 2008, Boundary Control of PDEs: A Course on Backstepping Designs, SIAM, Philadelphia, PA.
[26] Hale, J. K., and Lunel, S. M. V., 1990, "Averaging in Infinite Dimensions," J. Integral Equations Appl., 2(4), pp. 463–494.
[27] Oliveira, T. R., and Krstic, M., 2019, "Compensation of Wave PDEs in Actuator Dynamics for Extremum Seeking Feedback," 13th IFAC Workshop on Adaptive and Learning Control Systems, Winchester, UK, Dec. 4–6, pp. 134–139.
[28] Khalil, H. K., 2002, Nonlinear Systems, Prentice Hall, Upper Saddle River, NJ.
[29] Karafyllis, I., and Krstic, M., 2018, Input-to-State Stability for PDEs, Springer, Cham, Switzerland.
[30] Susto, G. A., and Krstic, M., 2010, "Control of PDE–ODE Cascades With Neumann Interconnections," J. Franklin Inst., 347(1), pp. 284–314.
[31] Ghaffari, A., Krstić, M., and Nešić, D., 2012, "Multivariable Newton-Based Extremum Seeking," Automatica, 48(8), pp. 1759–1767.
[32] Krstic, M., 2009, Delay Compensation for Nonlinear, Adaptive, and PDE Systems, Birkhauser, Boston, MA.
[33] Datko, R., Lagnese, J., and Polis, M. P., 1986, "An Example on the Effect of Time Delays in Boundary Feedback Stabilization of Wave Equations," SIAM J. Control Optim., 24(1), pp. 152–156.
[34] Liu, S.-J., and Krstic, M., 2010, "Stochastic Averaging in Continuous Time and Its Applications to Extremum Seeking," IEEE Trans. Automat. Control, 55(10), pp. 2235–2250.
[35] Ariyur, K., and Krstić, M., 2003, Real Time Optimization by Extremum Seeking Control, Wiley, Hoboken, NJ.

[36] Wang, L., Chen, S., and Ma, K., 2016, "On Stability and Application of Extremum Seeking Control Without Steady-State Oscillation," Automatica, **68**(6), pp. 18–26.

[37] Moura, S. J., and Chang, Y. A., 2013, "Lyapunov-Based Switched Extremum Seeking for Photovoltaic Power Maximization," Control Eng. Pract., **21**(7), pp. 971–980.

[38] Scheinker, A., and Krstić, M., 2014, "Extremum Seeking With Bounded Update Rates," Syst. Control Lett., **63**(1), pp. 25–31.

[39] Durr, H. B., Stankovic, M. S., Ebenbauer, C., and Johansson, K. H., 2013, "Lie Bracket Approximation of Extremum Seeking Systems," Automatica, **49**(6), pp. 1538–1552.

[40] Grushkovskaya, V., Zuyev, A., and Ebenbauer, C., 2018, "On a Class of Generating Vector Fields for the Extremum Seeking Problem: Lie Bracket Approximation and Stability Properties," Automatica, **94**(8), pp. 151–160.

[41] Oliveira, T. R., Feiling, J., Koga, S., and Krstic, M., 2020, "Multivariable Extremum Seeking for PDE Dynamic Systems," IEEE Trans. Automat. Control, pp. 1–8.